IL NUOVO CIMENTO Vol. 33 C, N. 5 Settembre-Ottobre 2010
DOI 10.1393/ncc/i2011-10737-9

Colloquia: LaThuile10

Search for neutral Higgs bosons decaying into four taus at LEP2

P. Spagnolo

INFN, Sezione di Pisa - Pisa, Italy
CERN - Geneva, Switzerland

(ricevuto il 14 Settembre 2010; pubblicato online il 14 Gennaio 2011)

Summary. — A search for the production and non-standard decay of a Higgs boson, h, into four taus through intermediate pseudoscalars, a, is conducted on $683\,\mathrm{pb}^{-1}$ of data collected by the ALEPH experiment at centre-of-mass energies from 183 to 209 GeV. No excess of events above background is observed, and exclusion limits are placed on the combined production cross section times branching ratio, $\xi^2 = \frac{\sigma(\mathrm{e^+e^-\to Zh})}{\sigma_{\mathrm{SM}}(\mathrm{e^+e^-\to Zh})} \times B(\mathrm{h}\to\mathrm{aa}) \times B(\mathrm{a}\to\tau^+\tau^-)^2$. For $m_\mathrm{h} < 107\,\mathrm{GeV}/c^2$ and $4 < m_\mathrm{a} < 10\,\mathrm{GeV}/c^2$, $\xi^2 > 1$ is excluded at the 95% confidence level.

PACS 14.80.Ec – Other neutral Higgs bosons.

1. – Introduction

Searches conducted at LEP2 have excluded the standard model (SM) Higgs boson decaying into $\mathrm{b\bar{b}}$ or $\tau^+\tau^-$ for masses below $114.4\,\mathrm{GeV}/c^2$ [1]. The LEP experiments observed a $\sim 2.5\sigma$ excess in the $\mathrm{b\bar{b}}$ final state for a Higgs boson mass around $100\,\mathrm{GeV}/c^2$, which is consistent with SM-like production and a reduced branching ratio into $\mathrm{b\bar{b}}$ [2]. This excess, the mild tension with electroweak precision tests [3], and the fine-tuning needed in the minimal supersymmetric standard model (MSSM) have prompted the consideration of models with exotic Higgs boson decays, such as those of the next-to-minimal supersymmetric standard model (NMSSM) [4,5] as well as more general frameworks [6,7]. In these models, new decay channels can dominate over $\mathrm{h}\to\mathrm{b\bar{b}}$ and render the Higgs boson "invisible" for conventional searches. In particular, a Higgs boson decaying into two light pseudoscalars is well motivated by these models and results in a four-body final state as the pseudoscalars decay into light fermions. A search for $\mathrm{h}\to 2\mathrm{a}\to 4\tau$ with ALEPH data, extending the mass range to $m_\mathrm{h} \approx 110\,\mathrm{GeV}/c^2$, is presented in this paper. The pseudoscalar a may arise from a two-higgs doublet model, as in the MSSM, or it can include a component from an additional singlet field as in the NMSSM. These possibilities differ in their details and relations between model parameters. The present search is performed in a model-independent manner and simply adopts the two main characteristics of the pseudoscalar: the coupling to a Higgs boson resulting in $\mathrm{h}\to\mathrm{aa}$

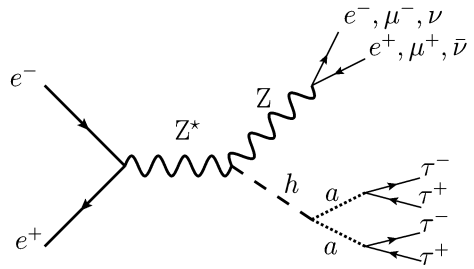

Fig. 1. – Higgs boson production and decay modes considered in this analysis.

decay and the coupling to SM fermions proportional to their Yukawa couplings. The present analysis concentrates on the region $2m_\tau < m_\mathrm{a} < 2m_\mathrm{b}$, where the $\mathrm{a} \to \tau^+\tau^-$ decay mode is expected to be substantial. The Higgs boson production mode considered here is the higgsstrahlung process, shown in fig. 1 with $\mathrm{Z} \to \mathrm{e}^+\mathrm{e}^-$, $\mu^+\mu^-$, $\nu\bar{\nu}$.

A detailed description of the ALEPH detector can be found in ref. [8]. The detector's performance is described in ref. [9]. The average centre-of-mass energies at which the machine operated and the corresponding integrated luminosities used in this analysis are presented in table I.

2. – Signal and background generation

Both signal and background were generated for all centre-of-mass energies shown in table I using the GEANT3-based simulation of ALEPH [10]. Backgrounds were generated with a variety of generators listed in table II.

3. – Event selection

For the mass range considered, the Higgs boson is produced approximately at rest, and thus the decay $\mathrm{h} \to 2\mathrm{a} \to 4\tau$ results in a pair of taus recoiling against another pair of taus. The JADE algorithm [20,21] was employed to cluster into jets all energy-flow objects except for those identified as energetic, isolated photons, energy deposits in the LCAL and SICAL, and the two hardest, oppositely-charged leptons in the case of the $\mathrm{Z} \to \ell^+\ell^-$ channels. Given that each jet is expected to arise from the on-shell decay $\mathrm{a} \to \tau^+\tau^-$, an effective way to target the signal topology is to use the JADE algorithm with y_cut chosen to merge proto-jets up to a mass of $m_\mathrm{jet} = 15\,\mathrm{GeV}/c^2$. Because the taus from the same a decay are highly collimated, the identification of jets containing the decay products of two taus was based only on the track multiplicity of the jets, denoted n_i^track, with the index i ordered in decreasing jet energy. Because the tau predominantly decays either to one charged particle ("one-prong" decay) or three charged particles ("three-prong" decay), each jet is expected to contain two, four, or six tracks. To maximize the tracking efficiency, the jets were required to be well contained in the tracking volume.

TABLE I. – *Integrated luminosities collected at the different average centre-of-mass energies.*

E_CM(GeV)	182.65	188.63	191.58	195.52	199.52	201.62	204.86	206.53
$\int \mathcal{L}\mathrm{d}t(\mathrm{pb}^{-1})$	56.8	174.2	28.9	79.9	86.3	41.9	81.4	133.2

TABLE II. – *Details on SM background processes and their categorisation. Fragmentation, hadronisation and final state radiation were simulated with* PYTHIA 6.1 [11]. PHOTOS [12] *was used to model final state radiation, and* TAUOLA [13] *was used for tau decays. More details can be found in ref.* [14].

Category	Process	Software
2f	$e^+e^- \to Z/\gamma^* \to q\bar{q}(\gamma)$	KK 4.14 [15]
	Bhabha and $e^+e^- \to Z/\gamma^* \to e^+e^-(\gamma)$	BHWIDE 1.01 [16]
	$e^+e^- \to Z/\gamma^* \to \mu^+\mu^-(\gamma)$	KK 4.14 [15]
	$e^+e^- \to Z/\gamma^* \to \tau^+\tau^-(\gamma)$	KK 4.14 [15]
	$e^+e^- \to Z \to \nu\bar{\nu}(\gamma)$	PYTHIA 6.1 [11]
4f	$e^+e^- \to Z/\gamma^* \to W^+W^-$	KORALW 1.51 [17]
	$e^+e^- \to ZZ$	PYTHIA 6.1 [11]
	$e^+e^- \to Z\,e^+e^-$	PYTHIA 6.1 [11]
	$e^+e^- \to Z\,\nu\bar{\nu}$	PYTHIA 6.1 [11]
	$e^+e^- \to W^\pm e^\mp \nu$	PYTHIA 6.1 [11]
$\gamma\gamma$	$\gamma\gamma \to \ell^+\ell^-$	PHOT02 [18, 19]
	$\gamma\gamma \to q\bar{q}$	PHOT02 [18, 19]
$n\gamma$	$e^+e^- \to n\gamma$	PYTHIA 6.1 [11]

The $Z \to \ell^+\ell^-$ decay is often accompanied by additional photons from final state radiation, which can carry substantial momentum. The photon was considered part of the candidate Z system when the invariant mass of the $\ell^+\ell^-\gamma$ system was closer to the Z mass than the invariant mass of the lepton pair alone. This algorithm resulted in an increase of $\sim 20\%$ in the signal efficiency after the Z mass window cut, $80 < m_Z < 102\,\mathrm{GeV}/c^2$. For each of the channels below, a loose selection and final selection are presented. The loose selection isolates the broad characteristics of the signal events and allows for comparison of the data and simulated backgrounds.

3˙1. $Z \to \ell^+\ell^-$. – The loose selection consisted of the following requirements. An e^+e^- or $\mu^+\mu^-$ pair and the presence of two jets (or 3 jets with $n_3^{\mathrm{track}} \leq 2$) were required for consistency with the final state of the signal. The three-jet events are kept to recover signal efficiency for events with converted photon arising from final state radiation. Proper containment of the jet in the tracking volume was ensured by requiring $|\cos\theta_{j_1}| < 0.9$ and $|\cos\theta_{j_2}| < 0.9$, where θ_{j_i} is the angle of the i-th jet with respect to the beam axis. Additional lepton isolation was imposed by requiring that a cone of 10° around each lepton contained less than 5% of the visible energy of the event and $\cos\theta_{jl}^{\mathrm{min}} < 0.95$, where $\theta_{jl}^{\mathrm{min}}$ is the minimum angle between each pairing of a jet and lepton.

The final selection consisted of the following requirements and maintained an acceptable signal efficiency while rejecting most backgrounds. A mass window for the candidate Z between 80–102 GeV/c^2 was effective at removing two-fermion backgrounds. Due to the neutrinos from tau decays the signal was separated from fully hadronic final states by requiring a missing energy $E_{\mathrm{mis}} > 20\,\mathrm{GeV}$. The expected jet configuration of the signal was enforced by requiring $\cos\theta_{j_1j_2} < 0$, where $\theta_{j_1j_2}$ is the angle between the two jets. Finally, the remaining backgrounds were suppressed by requiring $n_{1,2}^{\mathrm{track}} = 2$ or 4, the

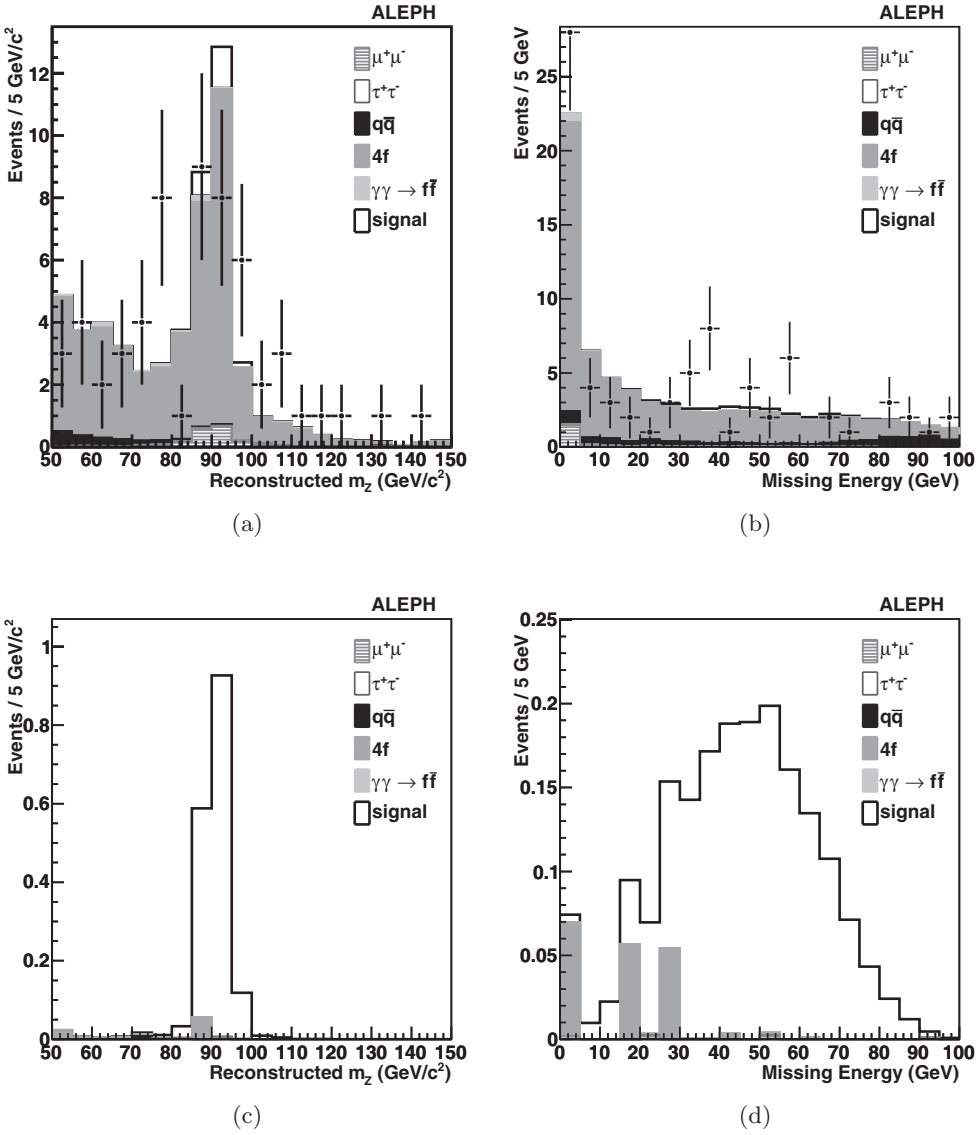

Fig. 2. – Distributions for the $Z \to \mu^+\mu^-$ channel after the loose selection for (a) the reconstructed Z invariant mass and (b) missing energy, where signal corresponds to $m_h = 100\,\mathrm{GeV}/c^2$, $m_a = 4\,\mathrm{GeV}/c^2$ with $\xi^2 = 1$. The same distributions are shown in (c) and (d) after the final selection, excluding any requirements on the variable shown.

dominant track multiplicities expected in the signal. Figures 2 show the distribution of the reconstructed Z mass and missing energy for the $Z \to \mu^+\mu^-$ channel. The numbers of events passing loose and final selection in data and simulated background are shown in table III.

TABLE III. – *Number of events passing loose and final selections in each channel, in data, simulated background, and simulated signal ($m_{\mathrm{h}} = 100$, $m_{\mathrm{a}} = 4\,GeV/c^2$). The numbers of events passing the final selection are categorised by track multiplicity.*

Channel	Selection $(n_1^{\mathrm{track}}, n_2^{\mathrm{track}})$	Data	Total background	Background category				Signal
				2f	4f	$\gamma\gamma$	nγ	
$\mathrm{Z} \to \mathrm{e}^+\mathrm{e}^-$	Loose	299	332	183	137	12.31	0.65	2.27
	(2,2)	0	0.034	0.034	0.000	0.000	0.000	0.689
	(2,4)+(4,2)	0	0.055	0.014	0.005	0.037	0.000	0.610
	(4,4)	0	0.031	0.019	0.013	0.000	0.000	0.126
$\mathrm{Z} \to \mu^+\mu^-$	Loose	83	74.50	12.79	60.64	1.07	0.00	2.37
	(2,2)	0	0.058	0.005	0.053	0.000	0.000	0.800
	(2,4)+(4,2)	0	0.005	0.000	0.005	0.000	0.000	0.676
	(2,2)	0	0.006	0.000	0.006	0.000	0.000	0.127
$\mathrm{Z} \to \nu\bar{\nu}$	Loose	206	200	135	47.97	13.50	3.74	12.63
	(2,2)	0	1.312	0.663	0.408	0.240	0.000	5.097
	(2,4)+(4,2)	0	1.948	0.528	0.575	0.845	0.000	4.741
	(4,4)	2	2.569	0.461	0.820	1.288	0.000	1.089

3˙2. $\mathrm{Z} \to \nu\bar{\nu}$. – All objects found in the event were clustered into jets as described above. The loose selection consisted of the following requirements. Missing energy greater than 30 GeV and missing mass, m_{mis}, greater than $20\,\mathrm{GeV}/c^2$ were used to reject dijet and other two-fermion backgrounds. In order to further reject the $\gamma\gamma$ background, events were required to have $E_{\mathrm{vis}} > 0.05\,E_{\mathrm{cm}}$ and $|\cos\theta_{\mathrm{me}}| < 0.9$, where E_{vis} is the visible energy and θ_{me} is the angle between the missing momentum vector and the beam axis. Events were required to have two well-contained jets with $|\cos\theta_{\mathrm{j}}| < 0.85$, dijet invariant mass $m_{\mathrm{j_1j_2}} > 10\,\mathrm{GeV}/c^2$, dijet angular separation $\cos\theta_{\mathrm{j_1j_2}} < 0$, and the highest energy jet was required to have $E_{\mathrm{j_1}} > 25\,\mathrm{GeV}$ and $n_1^{\mathrm{track}} = 2$ or 4.

The final selection consisted of the following requirements. First, the requirement $E_{\mathrm{j_1}} + E_{\mathrm{j_2}} + E_{\mathrm{mis}} > E_{\mathrm{cm}} - 5\,\mathrm{GeV}$ was used to reject events with energy deposits in the forward regions of the detector. Consistency with $\mathrm{Z} \to \nu\bar{\nu}$ was ensured by requiring $E_{\mathrm{mis}} > 60\,\mathrm{GeV}$ and $m_{\mathrm{mis}} > 90\,\mathrm{GeV}/c^2$. Finally, the second jet was also required to have $n_2^{\mathrm{track}} = 2$ or 4. The numbers of events passing loose and final selection in data and simulated background are shown in table III.

3˙3. *Signal efficiency*. – The $\mathrm{h} \to 2\mathrm{a} \to 4\tau$ signal efficiency is shown in fig. 3 as a function of the Higgs boson mass with $m_{\mathrm{a}} = 4$–$10\,\mathrm{GeV}/c^2$ for the three Z decay channels considered.

4. – Systematic uncertainties

Uncertainties and inaccuracies in the Monte Carlo simulation lead to systematic effects in the analysis. The impact of uncertainties in jet energy and direction, missing energy, and lepton identification and isolation were estimated. For the $\mathrm{Z} \to \ell^+\ell^-$ channels, the total relative systematic uncertainties from lepton identification and isolation were found to be 0.6%, 2.6% and 7.5% for the signal, ZZ, and Zee backgrounds, respectively. The systematic uncertainties for WW, Weν, q$\bar{\mathrm{q}}$, and other backgrounds were all smaller than

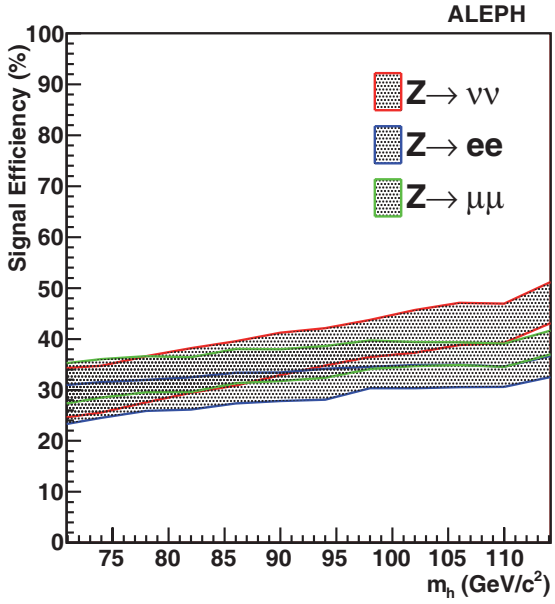

Fig. 3. – Signal efficiency as a function of the Higgs boson mass for the three channels considered in this work, $Z \to e^+e^-$, $\mu^+\mu^-$, and $\nu\bar{\nu}$. The upper (lower) portion of the efficiency band corresponds to $m_a = 4\ (10)\,\mathrm{GeV}/c^2$.

30%. Based on these estimates and the background composition, a 10% uncertainty is estimated for the background in the $Z \to \ell^+\ell^-$ channels. The agreement between the background estimate and the observed number of events in data with the loose selection is within the systematic and statistical uncertainty for all three channels. Given the low numbers of selected events, the final measurements are statistically limited.

5. – Results

No excess of events above the background was observed. Limits on the cross section times branching ratio with respect to the SM higgsstrahlung production cross section, $\xi^2 = \frac{\sigma(e^+e^-\to Zh)}{\sigma_{SM}(e^+e^-\to Zh)} \times B(h \to aa) \times B(a \to \tau^+\tau^-)^2$ were determined. Figure 4a shows the 95% confidence level upper-limit on ξ^2 as a function of m_h for $m_a = 10\,\mathrm{GeV}/c^2$. Figure 4b shows 95% confidence level contours of ξ^2 in the (m_h, m_a)-plane. Because the selection has no m_h or m_a dependence, the resulting upper limits are fully correlated. The observed number of events is consistent with a downward fluctuation of the background, which leads to stronger than expected limits on ξ^2.

6. – Conclusions

A search for a Higgs boson produced via higgsstrahlung at LEP2 energies has been performed, where $h \to 2a \to 4\tau$ and $Z \to e^+e^-$, $\mu^+\mu^-$, $\nu\bar{\nu}$. No evidence for an excess of events above background was observed, and a limit on the combined production cross section times branching ratio, $\xi^2 = \frac{\sigma(e^+e^-\to Zh)}{\sigma_{SM}(e^+e^-\to Zh)} \times B(h \to aa) \times B(a \to \tau^+\tau^-)^2$ is

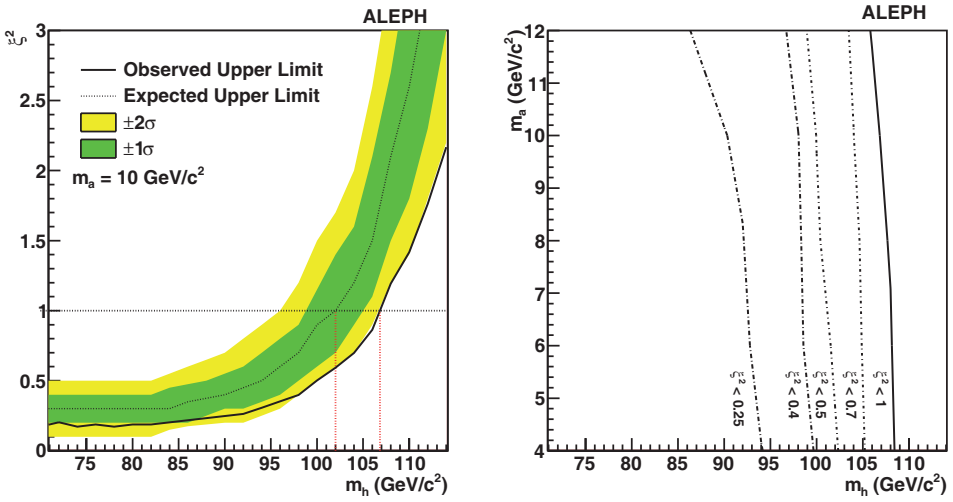

(a) (b)

Fig. 4. – (a) Observed and expected 95% confidence level limit on ξ^2 as a function of the Higgs boson mass for $m_{\mathrm{a}} = 10\,\mathrm{GeV}/c^2$. (b) Contours of observed 95% confidence level limit on ξ^2 in the $(m_{\mathrm{h}}, m_{\mathrm{a}})$-plane.

presented. For $m_{\mathrm{h}} < 107\,\mathrm{GeV}/c^2$ and $4 < m_{\mathrm{a}} < 10\,\mathrm{GeV}/c^2$, $\xi^2 > 1$ is excluded at the 95% confidence level. This analysis covers a region of parameter space previously left unexplored, and further constrains models with non-standard Higgs decays, such as the NMSSM.

* * *

I wish to thank J. Beacham, K. Stuart Cranmer and I. Yavin for the impressive work, N. Weiner and R. Barbieri for the encouragement and motivation, and all the ALEPH Collaboration for the support.

REFERENCES

[1] The LEP Working Group for Higgs Boson Searches, ALEPH, DELPHI, L3, and OPAL Collaborations, *Phys. Lett. B*, **565** (2003) 61, [hep-ex/0306033].
[2] The LEP Working Group for Higgs Boson Searches, ALEPH, DELPHI, L3, and OPAL Collaborations, *Eur. Phys. J. C*, **47** (2006) 547, [hep-ex/0602042].
[3] Barbieri R. and Strumia A., *Phys. Lett. B*, **462** (1999) 144, [hep-ph/9905281].
[4] Dermisek R. and Gunion J. F., *Phys. Rev. Lett.*, **95** (2005) 041801, [hep-ph/0502105].
[5] Dermisek R. and Gunion J. F., *Phys. Rev. D*, **76** (2007) 095006, [arXiv:0705.4387].
[6] Chang S., Fox P. J. and Weiner N., *JHEP*, **08** (2006) 068, [hep-ph/0511250].
[7] Chang S., Dermisek R., Gunion J. F. and Weiner N., *Annu. Rev. Nucl. Part. Sci.*, **58** (2008) 75, [arXiv:0801.4554].
[8] The ALEPH Collaboration, *Nucl. Instrum. Methods A*, **294** (1990) 121.
[9] The ALEPH Collaboration, *Nucl. Instrum. Methods A*, **360** (1995) 481.
[10] Brun R. *et al.*, CERN Internal Report No. CERN DD/EE/84-1 (1987).
[11] Sjöstrand T. *et al.*, *Comput. Phys. Commun.*, **135** (2001) 238, [hep-ph/0010017].
[12] Barberio E. and Was Z., *Comput. Phys. Commun.*, **79** (1994) 291.

[13] Jadach S., Was Z., Decker R. and Kuhn J. H., *Comput. Phys. Commun.*, **76** (1993) 361.
[14] The ALEPH Collaboration, *Eur. Phys. J. C*, **38** (2004) 147.
[15] Jadach S., Ward B. F. L. and Was Z., *Comput. Phys. Commun.*, **130** (2000) 260, [hep-ph/9912214].
[16] Jadach S., Placzek W. and Ward B. F. L., *Phys. Lett. B*, **390** (1997) 298, [hep-ph/9608412].
[17] Jadach S., Placzek W., Skrzypek M., Ward B. F. L. and Was Z., *Comput. Phys. Commun.*, **140** (2001) 475, [hep-ph/0104049].
[18] Vermaseren J. A. M., *Proceedings of the IV International Workshop on Gamma Gamma Interactions*, edited by Cochard G. and Kessler P. (1980).
[19] The ALEPH Collaboration, *Phys. Lett. B*, **313** (1993) 509.
[20] The JADE Collaboration, *Z. Phys. C*, **33** (1987) 339.
[21] The JADE Collaboration, *Phys. Lett. B*, **213** (1988) 235.